$P < 0.05$ for multiple comparisons. In a separate session, ERPs were sampled at 125 Hz with a 128-electrode geodesic sensor net reference to the vertex [D. Tucker, *Electroencephalogr. Clin. Neurophysiol.* **87**, 154 (1993)]. We rejected trials with incorrect responses, voltages exceeding ±100 μV, transients exceeding ±50 μV, electro-oculogram activity exceeding ±70 μV, or response times outside a 200- to 2500-ms interval. The remaining trials were averaged in synchrony with stimulus onset, digitally transformed to an average reference, band-pass filtered (0.5 to 20 Hz), and corrected for baseline over a 200-ms window before stimulus onset. Experimental conditions were compared within the first 400 ms by sample-by-sample *t* tests, with a criterion of $P < 0.05$ for five consecutive samples on at least eight electrodes simultaneously. Two-dimensional maps of scalp voltage were constructed by spherical spline interpolation [F. Perrin, J. Pernier, D. Bertrand, J. F. Echallier, *Electroencephalogr. Clin. Neurophysiol.* **72**, 184 (1989)]. Dipole models were generated with BESA [M. Scherg and P. Berg, *BESA—Brain Electric Source Analysis Handbook* (Max-Planck Institute for Psychiatry, Munich, 1990)]. Three fixed dipoles were placed at locations suggested by fMRI (left inferior frontal and bilateral parietal), and the program selected the dipole orientation and strength to match the exact-approximate ERP difference on a 216- to 280-ms time window, during which significant differences were found.

13. A. R. Damasio and N. Geschwind, *Annu. Rev. Neurosci.* **7**, 127 (1984); C. Price, *Trends Cogn. Sci.* **2**, 281 (1998).
14. R. A. Andersen, *Philos. Trans. R. Soc. London Ser. B* **352**, 1421 (1997); A. Berthoz, *ibid.*, p. 1437; M. Jeannerod, *The Cognitive Neuroscience of Action* (Blackwell, New York, 1997); L. H. Snyder, K. L. Grieve, P. Brotchie, R. A. Andersen, *Nature* **394**, 887 (1998).
15. R. Kawashima *et al.*, *Neuroreport* **7**, 1253 (1996); H. Sakata and M. Taira, *Curr. Biol.* **4**, 847 (1994).
16. H. Kawamichi, Y. Kikuchi, H. Endo, T. Takeda, S. Yoshizawa, *Neuroreport* **9**, 1127 (1998); S. M. Kosslyn, G. J. DiGirolamo, W. L. Thompson, N. M. Alpert, *Psychophysiology* **35**, 151 (1998); W. Richter, K. Ugurbil, A. Georgopoulos, S. G. Kim, *Neuroreport* **8**, 3697 (1997).
17. M. Corbetta, F. M. Miezin, G. L. Schulman, S. E. Petersen, *J. Neurosci.* **13**, 1202 (1993); M. Corbetta, G. L. Shulman, F. M. Miezin, S. E. Petersen, *Science* **270**, 802 (1995); A. C. Nobre *et al.*, *Brain* **120**, 515 (1997); M. I. Posner and S. Dehaene, *Trends Neurosci.* **17**, 75 (1994).
18. S. Dehaene, *J. Cogn. Neurosci.* **8**, 47 (1996); S. Dehaene *et al.*, *Neuropsychologia* **34**, 1097 (1996); P. E. Roland and L. Friberg, *J. Neurophysiol.* **53**, 1219 (1985); L. Rueckert *et al.*, *Neuroimage* **3**, 97 (1996).
19. The exact and approximate tasks did not differ in mean response time (fMRI: 772 and 783 ms; ERPs: 913 and 946 ms, respectively) nor in error rate (fMRI: 4.4 and 5.3%; ERPs: 2.7 and 2.3%, respectively) (all $Fs < 1$).
20. In individual analyses ($P < 10^{-3}$, corrected), the finding of greater intraparietal activation during approximation than during exact addition was replicated in five of seven subjects, whereas significantly greater left inferior frontal activation during exact addition was observed in four of seven subjects.
21. S. E. Petersen, P. T. Fox, M. I. Posner, M. Mintun, M. E. Raichle, *Nature* **331**, 585 (1988); M. E. Raichle *et al.*, *Cereb. Cortex* **4**, 8 (1994); R. Vandenberghe, C. Price, R. Wise, O. Josephs, R. S. J. Frackowiak, *Nature* **383**, 254 (1996); A. D. Wagner *et al.*, *Science* **281**, 1188 (1998).
22. Y. G. Abdullaev and N. P. Bechtereva, *Int. J. Psychophysiol.* **14**, 167 (1993); Y. G. Abdullaev and M. I. Posner, *Neuroimage* **7**, 1 (1998); A. Z. Snyder, Y. G. Abdullaev, M. I. Posner, M. E. Raichle, *Proc. Natl. Acad. Sci. U.S.A.* **92**, 1689 (1995).
23. H. Hécaen, R. Angelergues, S. Houillier, *Rev. Neurol.* **105**, 85 (1961); M. Rosselli and A. Ardila, *Neuropsychologia* **27**, 607 (1989).
24. S. Dehaene and L. Cohen, *Cortex* **33**, 219 (1997).
25. A. L. Benton, *Arch. Neurol.* **49**, 445 (1992); Y. Takayama, M. Sugishita, I. Akiguchi, J. Kimura, *ibid.* **51**, 286 (1994); M. Delazer and T. Benke, *Cortex* **33**, 697 (1997). Note that in such left parietal cases, the preservation of exact arithmetic facts is clearest for very small multiplication and addition problems (*23*). As the numbers involved in an exact arithmetic problem get larger, subjects are more and more likely to rely on quantity-based strategies to supplement rote verbal retrieval [(*7*); see also J. A. LeFevre *et al.*, *J. Exp. Psychol. Gen.* **125**, 284 (1996); J. LeFevre, G. S. Sadesky, J. Bisanz, *J. Exp. Psychol. Learn. Mem. Cogn.* **22**, 216 (1996)]. Indeed, supplementary fMRI analyses (available from S. Dehaene) showed that, within the present exact addition task, increasing problem sizes caused greater activation of the bilateral intraparietal circuit in regions identical to those active during approximation. This finding suggests that verbal and quantity representations of numbers are functionally integrated in the adult brain. Although only the verbal circuit is used for well-rehearsed exact arithmetic facts, both circuits are used when attempting to retrieve lesser-known facts.
26. S. Dehaene and L. Cohen, *Neuropsychologia* **29**, 1045 (1991).
27. T. Dantzig, *Number: The Language of Science* (Free Press, New York, 1967); G. Ifrah, *Histoire Universelle des Chiffres* (Robert Laffont, Paris, 1994).
28. M. Kline, *Mathematical Thought from Ancient to Modern Times* (Oxford Univ. Press, New York, 1972).
29. S. T. Boysen and E. J. Capaldi, Eds., *The Development of Numerical Competence: Animal and Human Models* (Erlbaum, Hillsdale, NJ, 1993); E. M. Brannon and H. S. Terrace, *Science* **282**, 746 (1998); S. Dehaene, G. Dehaene-Lambertz, L. Cohen, *Trends Neurosci.* **21**, 355 (1998); C. R. Gallistel, *Annu. Rev. Psychol.* **40**, 155 (1989).
30. K. Wynn, *Trends Cogn. Sci.* **2**, 296 (1998).
31. S. Dehaene, *The Number Sense* (Oxford Univ. Press, New York, 1997).

32. Supported by NIH grant HD23103 (E.S.) and by the Fondation pour la Recherche Médicale (S.D.). We gratefully acknowledge discussions with L. Cohen, D. Le Bihan, J.-B. Poline, and N. Kanwisher.

6 January 1999; accepted 16 March 1999

Discovery of a Small Molecule Insulin Mimetic with Antidiabetic Activity in Mice

Bei Zhang,[1]* Gino Salituro,[2] Deborah Szalkowski,[1] Zhihua Li,[1] Yan Zhang,[2] Inmaculada Royo,[4] Dolores Vilella,[4] Maria Teresa Díez,[4] Fernando Pelaez,[4] Caroline Ruby,[2] Richard L. Kendall,[5] Xianzhi Mao,[5] Patrick Griffin,[3] Jimmy Calaycay,[3] Juleen R. Zierath,[6] James V. Heck,[2] Roy G. Smith,[1]† David E. Moller[1]

Insulin elicits a spectrum of biological responses by binding to its cell surface receptor. In a screen for small molecules that activate the human insulin receptor tyrosine kinase, a nonpeptidyl fungal metabolite (L-783,281) was identified that acted as an insulin mimetic in several biochemical and cellular assays. The compound was selective for insulin receptor versus insulin-like growth factor I (IGFI) receptor and other receptor tyrosine kinases. Oral administration of L-783,281 to two mouse models of diabetes resulted in significant lowering in blood glucose levels. These results demonstrate the feasibility of discovering novel insulin receptor activators that may lead to new therapies for diabetes.

The actions of insulin are initiated by its binding to the insulin receptor (IR), a disulfide-bonded heterotetrameric membrane protein (*1–3*). Insulin binds to two asymmetric sites on the extracellular α subunits and causes conformational changes that lead to autophosphorylation of the membrane-spanning β subunits and activation of the receptor's intrinsic tyrosine kinase (*4*, *5*). Insulin receptors transphosphorylate several immediate substrates (on Tyr residues) including insulin receptor substrate (IRS) proteins (*6*). These events lead to the activation of downstream signaling molecules. The function of the receptor tyrosine kinase is essential for the biological effects of insulin (*1–6*).

The pathogenesis of type 2, non–insulin-dependent diabetes mellitus (NIDDM) is complex, involving progressive development of insulin resistance and a defect in insulin secretion, which leads to overt hyperglycemia. The molecular basis for insulin resistance in NIDDM remains poorly understood. However, several studies have shown modest (≈30 to 40%) decreases in IR number with tissues or cells from NIDDM patients (*7*).

[1]Department of Molecular Endocrinology, [2]Department of Natural Product Drug Discovery, [3]Department of Molecular Diversity and Design, Merck Research Laboratories, R80W250, Post Office Box 2000, Rahway, NJ 07065, USA. [4]Centro de Investigación Básica, Merck, Sharp & Dohme de España, S. A. Josefa Valcárcel 38, Madrid 28027, Spain. [5]Department of Cancer Research, Merck Research Laboratories, Post Office Box 4, West Point, PA 19486, USA. [6]Department of Clinical Physiology, Karolinska Hospital, Karolinska Institute, S-171 76 Stockholm, Sweden.

*To whom correspondence should be addressed. E-mail: bei_zhang@merck.com

†Present address: Huffington Center on Aging and Department of Cell Biology, Baylor College of Medicine, One Baylor Plaza, M-320, Houston, TX 77030, USA.

More importantly, substantial decreases in insulin-stimulated receptor tyrosine kinase activity and defects in receptor-mediated IRS phosphorylation or phosphatidylinositide (PI) 3-kinase activation have been found in muscle or fat tissue from NIDDM patients or rodent NIDDM models (*7*–*9*). Thus, a subset of NIDDM patients have clear defects in insulin signaling that, in theory, might be overcome by treatment aimed at augmenting IR function. Given that most NIDDM patients respond to insulin secretagogues (sulfonylureas) or to moderate doses of exogenous insulin, new approaches that mimic insulin's effects or augment the effect of residual endogenous insulin are likely to be beneficial. Because patients with type 1, insulin-dependent, diabetes depend on parenteral exogenous insulin injections for metabolic control, the discovery of orally active small molecules that mimic insulin's effects could eventually lead to alternative therapies for this disorder.

To identify small molecule IR activators, we designed a cell-based screening assay with Chinese hamster ovary cells that overexpress the human IR (CHO.IR) (*10*). After incubation of intact cells with insulin or test compounds, IR is immunopurified and assayed for tyrosine kinase (IRTK) activity toward an exogenous substrate. Through extensive screening of over 50,000 mixtures of synthetic compounds and natural products, we identified a small molecule (L-783,281) (Fig. 1A) from a fungal extract (*Pseudomassaria* sp.) that was reproducibly active in the assay (*11*). At concentrations of 3 to 6 μM, L-783,281 induced 50% of the maximal effect of insulin on IRTK activity (Fig. 1B). Substantial enhancement of insulin-stimulated IRTK activation was also observed at lower concentrations (0.6 to 2 μM) (Fig. 1C), consistent with the notion that L-783,281 can function as an insulin sensitizer. In contrast, a closely related natural product analog, L-767,827 (hinulliquinone), was ~100 times less active in the assay.

L-783,281 induced phosphorylation of the IR β subunit and IRS-1 in CHO.IR cells, as evidenced by anti-phosphotyrosine immunoblotting (Fig. 2A). In contrast, in CHO cells overexpressing the insulin-like growth factor receptor (CHO.IGFIR), L-783,281 (10 μM) did not stimulate IGFIR or IRS-1 tyrosyl

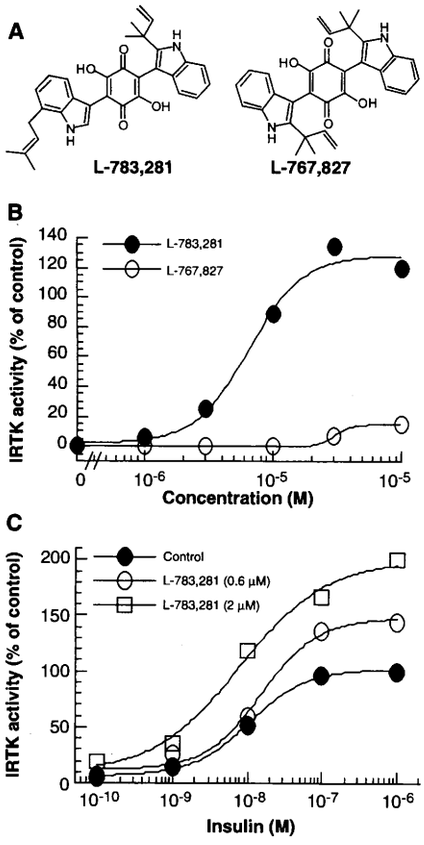

Fig. 1. (**A**) Structures and (**B** and **C**) effects on IRTK activity in CHO.IR cells. CHO.IR cells were cultured in 96-well plates (150,000 cells per well) for 24 hours and then serum-starved for 2 hours before treatment with test compounds or insulin in the presence of 0.1% dimethyl sulfoxide (DMSO) in the medium for 20 min at 37°C. Preparation of cell lysates, immunopurification of IR, and measurement of IRTK activity were performed as described (*23*). Receptors were captured with antibody to IR (Ab-3, Oncogene Science Diagnostics, Cambridge, Massachusetts), and IRTK activity was measured with [γ -^{32}P]ATP and poly(Glu:Tyr) (4:1) as substrate. The activities of test compounds were expressed as a percentage of the maximal activity achieved with 100 nM insulin. (B) Dose-response curves for L-783,281 and L-767,827. (C) Cells were treated with insulin in the absence or presence of L-783,281.

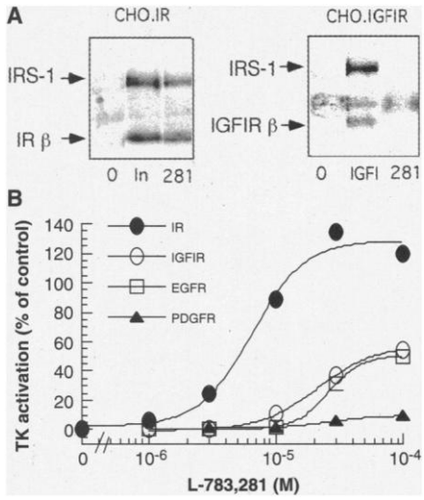

Fig. 2. Selectivity of L-783,281. (**A**) Tyrosine phosphorylation of IRS-1 and β subunits of IR or IGFIR (*23*). CHO.IR or CHO.IGFIR cells were left untreated (0), or treated with insulin (In) (10 nM), IGFI (100 nM), or 10 μM L-783,281 (281). Proteins were separated by electrophoresis, blotted onto a membrane, and detected with an antibody to phosphotyrosine (PY20, Transduction Laboratories, Lexington, Kentucky). (**B**) Activation of RTKs by L-783,281 in CHO.IR, CHO.IGFIR, CHO.EGFR, or CHO.PDGFR cells. Cells were treated with L-783,281 or cognate receptor ligands. The activity of L-783,281 was expressed as a percentage of control maximal activity (achieved with 100 nM insulin for IR, 100 nM IGFI for IGFIR, 10 nM EGF for EGFR, or 0.1 μg of PDGF per milliliter for PDGFR).

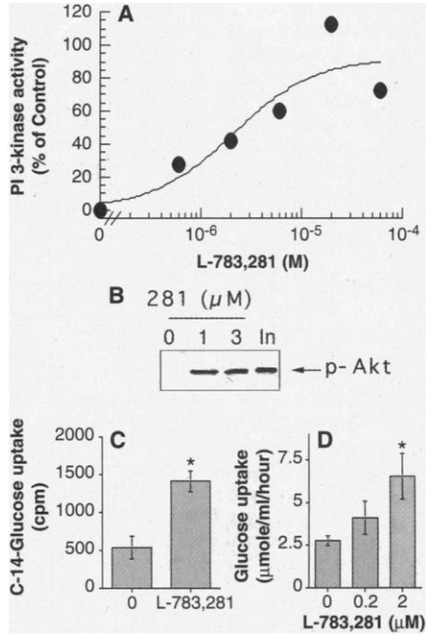

Fig. 3. Activation of the insulin signaling pathway in cells treated with L-783,281. (**A**) Activation of PI 3-kinase. CHO.IR cells were treated with L-783,281 or 100 nM insulin for 20 min or left untreated. Proteins from lysates were immunoprecipitated with an antibody to phosphotyrosine, and PI 3-kinase activity was measured (*23*). Activity is expressed as a percentage of control (100 nM insulin). (**B**) Phosphorylation of Akt. CHO.IR cells were treated with L-783,281 or 10 nM insulin for 20 min. Fractionated proteins were blotted onto a membrane and detected with an antibody specific for Phospho-Ser-473 of Akt (New England Biolabs, Beverly, Massachusetts). (**C**) Glucose uptake. Adipocytes from male Wistar rats were incubated with L-783,281 (10 μM) for 30 min. [^{14}C]Glucose was added, and the cells were further incubated for 5 min. [^{14}C]Glucose uptake by adipocytes was quantitated (*15*). In the same experiment, insulin (7 nM)-stimulated glucose uptake was 450% that of basal uptake. (**D**) Glucose uptake in intact soleus muscle from lean (C57BL6) mice (*16*). Tissue was first incubated with L-783,281 for 30 min and then with 1 mM 2-deoxy-[1,2,^{3}H]glucose (2.5 μCi/ml) and 19 mM [^{14}C]mannitol (0.35 μCi/ml) for 30 min. Muscles were then processed as described (*24*). In the same experiment, insulin-stimulated 2-deoxyglucose was 212 and 430% that of basal uptake, for 0.03 and 2.0 mU of insulin per milliliter, respectively. Shown are the mean ± SEM for each data point (at least triplicate determination). $^{*}P < 0.02$ (Student's *t* test).

phosphorylation. No other L-783,281–induced tyrosyl protein phosphorylation was evident, suggesting that the compound is selective for IR versus IGFIR activation. In subsequent studies in which quantitative tyrosine kinase or anti-phosphotyrosine enzyme-linked immunosorbent assays were applied to CHO.IGFIR cells and epidermal growth factor receptor–overexpressing cells (CHO.EGFR), respectively, L-783,281 was found to weakly activate IGFIR and EGFR at concentrations greater than 30 μM (Fig. 2B). In addition, L-783,281 did not induce EGFR activation (up to 60 μM) in a human epidermoid carcinoma cell line (A431) that expresses high levels of endogenous EGFR (*12*). The compound (up to 100 μM) also did not activate the platelet-derived growth factor receptor (PDGFR) in transfected CHO cells (Fig. 2B) or in fetal human foreskin fibroblasts, which express high levels of endogenous PDGFR (*12*).

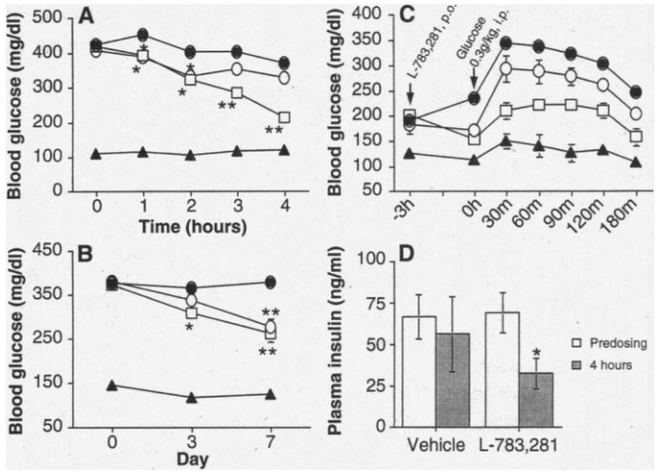

Fig. 4. Antidiabetic efficacy of orally administered L-783,281 in mouse models of diabetes. (**A**) Acute glucose lowering by L-783,281 in *db/db* mice. Nine-week-old male *db/db* mice (Jackson Labs) were orally treated (by gavage) with vehicle [0.5% methylcellulose (●)] or with single doses of L-783,281 [5 mg/kg (○) or 25 mg/kg (□)] followed by immediate removal of food. Mice had free access to water. Blood glucose was monitored before and after dosing at 1-hour intervals with a One Touch Glucometer (Lifescan, Milpitas, California). (▲) Lean control mice (not dosed). (**B**) Glucose lowering in *db/db* mice after long-term dosing. Eight-week-old male *db/db* mice were treated daily with an oral dose of vehicle (●) or L-783,281 [5 mg kg^{-1} day^{-1} (○) or 20 mg kg^{-1} day^{-1} (□)]. Mice were fed ad libitum. (▲) Lean control mice (not dosed). (**C**) Glucose tolerance test in *ob/ob* mice. Twelve-week-old male *ob/ob* mice (Jackson Labs) were orally dosed with vehicle or with a single dose of L-783,281 [5 mg/kg (○) or 20 mg/kg (□)] followed by immediate removal of food. Mice had free access to water. A bolus of glucose (0.3 gm/kg) was injected intraperitoneally 3 hours later. (▲) Lean control mice. (**D**) Plasma insulin level in 12-week-old *ob/ob* mice before and 4 hours after single oral dosing of L-783,281. Shown are the mean ± SEM for each data point (n = 7 to 9 for each group). In some instances SEMs are within the area of the symbols. $^{*}P < .05$; $^{**}P < 0.002$ (Student's t test). All animals were fed ad libitum before the study. Animal care was in accordance with institutional guidelines.

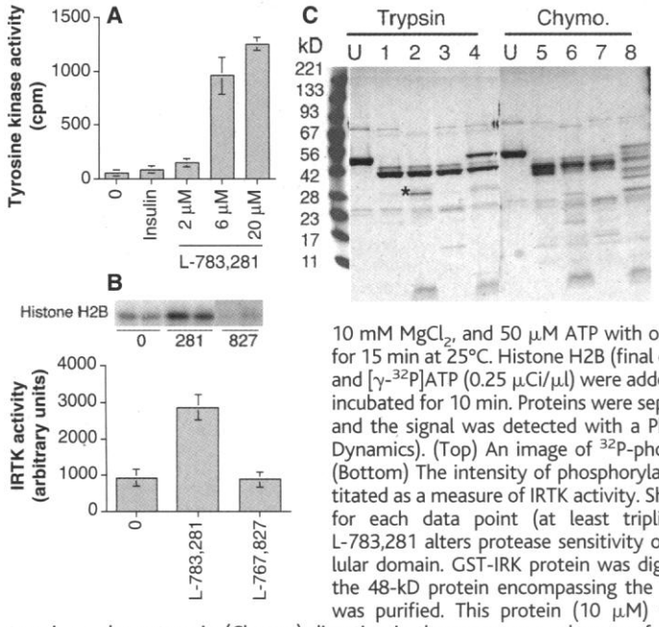

Fig. 5. Interaction of L-783,281 with intracellular domain of IR. (**A**) Activation of TK in CHO cells expressing an IRR/IR chimera. CHO.IRR/IR cells (*17*) were treated with 100 nM insulin or L-783,281 for 20 min. (**B**) In vitro activation of IRTK. Recombinant GST-IRK (*18*) was incubated with 50 mM tris-HCl (pH 7.4), 10 mM $MgCl_2$, and 50 μM ATP with or without test compounds for 15 min at 25°C. Histone H2B (final concentration 0.35 μg/ml) and [γ-^{32}P]ATP (0.25 μCi/μl) were added and the samples further incubated for 10 min. Proteins were separated by electrophoresis, and the signal was detected with a PhosphorImager (Molecular Dynamics). (Top) An image of ^{32}P-phosphorylated histone H2B. (Bottom) The intensity of phosphorylated H2B bands was quantitated as a measure of IRTK activity. Shown are the mean ± SEM for each data point (at least triplicate determination). (**C**) L-783,281 alters protease sensitivity of recombinant IR intracellular domain. GST-IRK protein was digested with thrombin, and the 48-kD protein encompassing the intracellular domain of IR was purified. This protein (10 μM) was subjected to limited trypsin or chymotrypsin (Chymo.) digestion in the presence or absence of compounds. The digestion mixtures were separated by electrophoresis and the gels were stained with Coomassie blue. U: undigested protein; lanes 1 and 5: DMSO control; lanes 2 and 6: 200 μM L-783,281; lanes 3 and 7: 5 mM ATP-γ-S; lanes 4 and 8: 200 μM L-783,281 plus 5 mM ATP. The asterisk indicates the 30-kD digestion product (see text).

In addition to stimulating IR-mediated IRS-1 phosphorylation, L-783,281 activated other components of the insulin signal transduction pathway. It stimulated PI 3-kinase activity (*13*) (Fig. 3A) and phosphorylation of Akt kinase (*14*) in CHO.IR cells (Fig. 3B). L-783,281 also stimulated glucose uptake in rat primary adipocytes (263% of basal level at 10 μM) (*15*) (Fig. 3C) and in isolated soleus muscle from lean mice (237% of basal level at 2 μM) (*16*) (Fig. 3D).

We next tested the in vivo efficacy of L-783,281 in *db/db* and *ob/ob* mice, two models of NIDDM. Single dose oral administration of L-783,281 resulted in dose-dependent lowering of blood glucose (Fig. 4A), with >50% transient correction of hyperglycemia achieved at 25 mg/kg (over 3 to 6 hours; food withheld). Long-term daily oral administration of L-783,281 (at 5 or 20 mg kg^{-1} day^{-1}) for 7 days also resulted in significant correction of hyperglycemia in *db/db* mice fed ad libitum (Fig. 4B). The effect of L-783,281 on blood glucose in *db/db* mice was independent of an effect on circulating glucagon (*12*) and independent of food intake. Administration of L-783,281 to *ob/ob* mice, which have extreme hyperinsulinemia and mild hyperglycemia, resulted in significant and dose-dependent improvement in glucose tolerance (Fig. 4C). Single oral doses of L-783,281 also suppressed elevated plasma insulin levels in *ob/ob* mice (Fig. 4D). Long-term treatment (up to 15 days) with therapeutic doses of L-783,281 did not affect food intake, body weight, organ weights, or blood chemistry (values of standard physiological indicators such as liver function were normal) (*12*).

We also investigated the mechanism of action of L-783,281. Several lines of evidence suggested that L-783,281 directly activates the IR intracellular β subunit (tyrosine kinase domain). First, in experiments with transfected CHO cells (CHO.IRR/IR), which overexpress chimeric receptors composed of the IR intracellular domain fused to the nonhomologous IR-related receptor (IRR) extracellular domain (*17*), L-783,281 (but not insulin) still activated the receptor tyrosine kinase activity (Fig. 5A). Second, L-783,281 did not

displace radiolabeled insulin binding to IRs expressed in intact CHO.IR cells, nor did it affect the affinity of insulin for the receptor (*12*). Third, L-783,281, but not L-767,827, increased IRTK activity of recombinant IR in vitro (*18*) (Fig. 5B). Finally, the partial proteolysis pattern of the IR intracellular domain (48 kD) was altered in the presence of L-783,281 (Fig. 5C). A different pattern of proteolysis was observed when the 48-kD protein was incubated with an adenosine 5′-triphosphate (ATP) analog (ATP-γ-S) that affects IR kinase conformation (*5*). Yet another pattern was observed when the 48-kD protein was incubated with both L-783,281 and ATP-γ-S. Of particular interest was a ~30-kD band produced when the 48-kD protein was incubated with L-783,281 followed by partial digestion with trypsin (lane 2, asterisk). In the absence of L-783,281, a 10 to 50 times higher concentration of trypsin was required to produce the ~30-kD product. NH_2-terminal peptide sequencing of the ~30-kD band revealed the sequence Thr^{1031}-Val-Asn-Glu-Ser-Ala-Ser-Leu (*19*). This peptide is immediately adjacent to Lys^{1030}, the residue involved in ATP binding to the active site of the IRTK domain (*2*, *20*). Thus, interaction of L-783,281 with the IR kinase domain appears to alter the conformation of the protein in the region encompassing the ATP binding site, resulting in the exposure of tryptic recognition site (or sites) adjacent to Lys^{1030}. On the basis of published crystal structures, conformational change in the kinase domain is required for the activation of the receptor (*4*, *5*). The results of our studies suggest that interaction of L-783,281 with IRTK alters the conformation of IRTK, leading to its activation.

The discovery of L-783,281 demonstrates that a small, nonpeptidyl molecule is capable of mimicking the in vitro and in vivo function of a protein hormone by interacting with and activating its receptor. Vanadate is another orally active compound that can function in vivo as an insulin mimetic agent (*21*). However, unlike vanadate, which augments tyrosyl phosphorylation of a wide variety of cellular proteins and functions in vitro as an inhibitor of protein tyrosine phosphatases (PTPases) (*22*), L-783,281 was selective for the IR and did not inhibit selected PTPases in vitro (*12*). Selective IR activators, as exemplified by L-783,281, may lead to the development of a novel class of antidiabetic agents.

References and Notes

1. O. M. Rosen, *Diabetes* **38**, 1508 (1989).
2. Y. Ebina *et al.*, *Cell* **40**, 747 (1985).
3. A. Ullrich *et al.*, *Nature* **313**, 756 (1985).
4. S. R. Hubbard, L. Wei, L. Ellis, W. A. Hendrickson, *ibid.* **372**, 746 (1994).
5. S. R. Hubbard, *EMBO J.* **16**, 5572 (1997).
6. M. F. White and C. R. Kahn, in *Insulin Resistance*, D. E. Moller, Ed. (Wiley, Chichester, UK, 1994), pp. 9–24.
7. B. L. Seely and J. M. Olefsky, in (*6*), pp. 187–252
8. L. J. Goodyear *et al.*, *J. Clin. Invest.* **95**, 2195 (1995).
9. J. F. Caro *et al.*, *ibid.* **79**, 1330 (1987).
10. Y. Ebina *et al.*, *Proc. Natl. Acad Sci. U.S.A.* **82**, 8014 (1985).
11. L-783,281 was isolated from liquid cultures of a strain of the fungus *Pseudomassaria* sp. (American Type Culture Collection 74411), which was recovered from leaves of an undetermined plant collected near Kinshasa, Democratic Republic of Congo. For production of the compound, the strain was grown in a medium containing (per liter) D-mannitol (100 g), NZ-Amine (type E) (Quest International, Norwich, NY) (33 g), Difco–Yeast Extract (Becton Dickinson, Franklin Lakes, NJ) (10 g), ammonium sulfate (5 g), and K_2HPO_4 (9 g). An organic extract of the fermentation broth was prepared by gel chromatography and two subsequent cycles of reversed-phase high-performance liquid chromatography. The title compound crystallized as dark purple needles from ethyl acetate:hexane when stored at 4°C. Spectroscopic data (^1H, ^{13}C, and two-dimensional nuclear magnetic resonance data and high-resolution fast atom bombardment mass spectroscopy) were collected on the pure compound, which was identified as demethylasterriquinone B-1 (L-783,281).
12. B. Zhang *et al.*, unpublished data.
13. G. Endemann, K, Yonezawa, R. A. Roth, *J. Biol. Chem.* **265**, 396 (1990); R. Levy-Toledano, M. Taouis, D. H. Blaettler, P. Gorden, S. Taylor, *ibid.* **269**, 31178 (1994).
14. T. F. Franke *et al.*, *Cell* **81**, 727 (1995).
15. B. B. Kahn, I. A. Simpson, S. W. Cushman, *J. Clin. Invest.* **82**, 691 (1988).
16. P. A. Hansen, E. A. Gulve, J. O. Holloszy, *J. Appl. Physiol.* **76**, 979 (1994).
17. B. Zhang and R. A. Roth, *J. Biol. Chem.* **267**, 18320 (1992).
18. The cytoplasmic domain of the human IR (Gln^{983} to the COOH-terminal stop codon) was cloned as an in-frame glutathione S-transferase fusion (GST-IRK) into the baculovirus expression vector pBlueBac 4.0 (Invitrogen, San Diego), and the resulting plasmid was transfected into Sf21 insect cells with the Bac-N-Blue Transfection Kit (Invitrogen). Recombinant virus was prepared and protein expressed as described [R. Kendall and K. Thomas, *Proc. Natl. Acad. Sci. U.S.A.* **90**, 10705 (1993)].
19. The trypsin digestion products were separated and visualized in 4 to 20% SDS-polyacrylamide gel stained with Coomassie blue. After electrotransfer onto a polyvinylidene difluoride membrane, the 30-kD protein was excised and subjected to automated Edman sequence analysis with a 477A sequenator (Applied Biosystems).
20. Y. Ebina *et al.*, *Proc. Natl. Acad Sci. U.S.A.* **84**, 704 (1987); C. K. Chou *et al.*, *J. Biol. Chem.* **262**, 1842 (1987); D. A. McClain *et al.*, *ibid.*, p. 14663.
21. J. Meyerovitch, Z. Farfel, J. Sack, Y. Shechter, *J. Biol. Chem.* **262**, 6658 (1987).
22. J. M. Denu, D. L. Kohse, J. Vijalakshmi, M. A. Saper, J. E. Dixon, *Proc. Natl. Acad. Sci. U.S.A.* **93**, 2493 (1996).
23. B. Zhang *et al.*, *J. Biol. Chem.* **269**, 25735 (1994).
24. H. Wallberg-Henriksson, N. Zetan, J. Henriksson, *ibid.* **262**, 7665 (1987).

25. We thank G. Bills, R. Schwartz, and L. So for characterization of the L-783,281–producing organism; D. Zink for mass spectroscopy data on L-783,281; T. Doebber, M. Wu, and J. Ryder for assistance with biological characterization; and M. Turner and S. Gould for invaluable support.

3 March 1999; accepted 2 April 1999

Roles of Phosphorylation Sites in Regulating Activity of the Transcription Factor Pho4

Arash Komeili and Erin K. O'Shea*

Transcription factors are often phosphorylated at multiple sites. Here it is shown that multiple phosphorylation sites on the budding yeast transcription factor Pho4 play distinct and separable roles in regulating the factor's activity. Phosphorylation of Pho4 at two sites promotes the factor's nuclear export and phosphorylation at a third site inhibits its nuclear import. Phosphorylation of a fourth site blocks the interaction of Pho4 with the transcription factor Pho2. Multiple phosphorylation sites provide overlapping and partially redundant layers of regulation that function to efficiently control the activity of Pho4.

Many signaling pathways rapidly and reversibly convert extracellular signals into changes in gene expression. Phosphorylation of a transcription factor, often at multiple sites, is a common mechanism for responding to signaling events (*1*). This modification can lead to changes in transcription factor concentration or activity in the nucleus (*2*). However, the role of multiple phosphorylation sites in regulating the activity of a protein is not well understood.

University of California–San Francisco, Department of Biochemistry and Biophysics, 513 Parnassus Avenue, San Francisco, CA 94143–0448, USA.

*To whom correspondence should be addressed. E-mail: oshea@biochem.ucsf.edu

To study how multiple phosphorylation sites control protein activity, we focused on the regulation of Pho4, a transcription factor in budding yeast that activates expression of genes induced in response to phosphate starvation (*3*). When yeast cells are grown in phosphate-rich conditions, Pho4 is phosphorylated by the Pho80/Pho85 cyclin-cyclin–dependent kinase (CDK) complex (*4*) and exported to the cytoplasm (*5*), thereby terminating expression of phosphate-responsive genes. The kinase Pho80/Pho85 phosphorylates Pho4 on five Ser-Pro (SP) dipeptides, referred to as SP1, SP2, SP3, SP4, and SP6 (*6*). When yeast cells are starved for phosphate, the CDK inhibitor Pho81 inactivates Pho80/Pho85 (*7*),